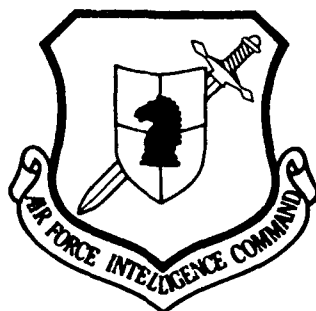


AD-A267 722



FASTC-ID(RS)T-0034-93

## FOREIGN AEROSPACE SCIENCE AND TECHNOLOGY CENTER



DTIC  
ELECTE  
AUG 11 1993  
S c D

EXPERIMENTAL STUDY OF VORTEX AND AERODYNAMIC  
CHARACTERISTICS OF STACK WINGS WITH SIDESLIP

by

Bao Guohua



93-18664



Approved for public release;  
Distribution unlimited.



# HUMAN TRANSLATION

FASTC-ID(RS)T-0034-93

20 July 1993

MICROFICHE NR: 93C000468

EXPERIMENTAL STUDY OF VORTEX AND AERODYNAMIC  
CHARACTERISTICS OF STACK WINGS WITH SIDESLIP

By: Bao Guohua

English pages: 10

Source: Kongqidonglixue Xuebao, Vol. 7, Nr. 2, June 1989;  
pp. 215-219

Country of origin: China

Translated by: Leo Kanner Associates  
F33657-88-D-2188

Requester: FASTC/TATV/Paul Freisthler

Approved for public release; Distribution unlimited.

DTIC QUALITY INSPECTED 3

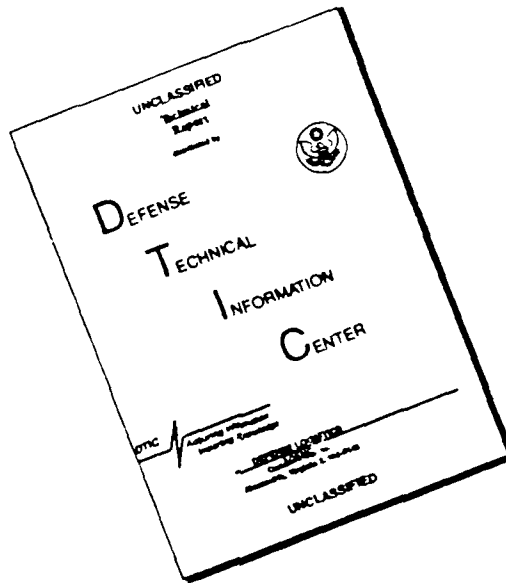
Accession For	
NTIS CRA&I	<input checked="" type="checkbox"/>
DTIC TAB	<input type="checkbox"/>
Unannounced	<input type="checkbox"/>
Justification	
By	
Distribution /	
Availability Codes	
Dist	Avail and/or Special

THIS TRANSLATION IS A RENDITION OF THE ORIGINAL FOREIGN TEXT WITHOUT ANY ANALYTICAL OR EDITORIAL COMMENT STATEMENTS OR THEORIES ADVOCATED OR IMPLIED ARE THOSE OF THE SOURCE AND DO NOT NECESSARILY REFLECT THE POSITION OR OPINION OF THE FOREIGN AEROSPACE SCIENCE AND TECHNOLOGY CENTER.

PREPARED BY:

TRANSLATION DIVISION  
FOREIGN AEROSPACE SCIENCE AND  
TECHNOLOGY CENTER  
WPAFB, OHIO

# DISCLAIMER NOTICE



THIS DOCUMENT IS BEST  
QUALITY AVAILABLE. THE COPY  
FURNISHED TO DTIC CONTAINED  
A SIGNIFICANT NUMBER OF  
PAGES WHICH DO NOT  
REPRODUCE LEGIBLY.

#### GRAPHICS DISCLAIMER

All figures, graphics, tables, equations, etc. merged into this translation were extracted from the best quality copy available.

EXPERIMENTAL STUDY OF VORTEX AND AERODYNAMIC  
CHARACTERISTICS OF STACK WINGS WITH SIDESLIP

Bao Guohua

Northwest Industrial University

**Abstract:** The paper reports on an experimental study of stack wings with small aspect ratio, and describes the variation of detached vortex system at the aircraft wing leading edge with different aspect ratios. The influence on aerodynamic characteristics due to vortex twisting and bursting is analyzed. As revealed in the study, sideslip delays the vortex twisting at the upstream side of the aircraft wing. The vortex bursts early. At the downward side, the phenomena are exactly in reverse. During sideslip, bursting of an asymmetrical vortex has an obvious influence on the aerodynamic characteristics.

**Keywords:** vortex, sideslip, stack wing, experiment.

## I. Introduction

After an airstream passes a long slender wing, the airstream separates along the leading edge of the aircraft wing and forms a detached leading-edge vortex on the wing surface. Induction of

the leading-edge vortex makes the characteristics of wing lift nonlinear. Most modern fighters adopt stack wings in order to utilize the beneficial interference of the leading-edge vortex to improve aircraft maneuverability characteristics. Much research was done on this point in China and abroad. As revealed in experiments, there are two leading-edge vortices on each half-wing at small angles of attack; these vortices originate, respectively, from the wing apex and the leading-edge angle of deflection (briefly referred to as the front vortex and the rear vortex). The front and rear vortices twist into each other and burst; this phenomenon strongly influences the wing's aerodynamic characteristics. When sideslip is present, as the leading-edge vortex is asymmetrical, it moves toward the lateral direction and bursts; this will have a significant effect on the aerodynamic characteristics of the wing, and especially its lateral characteristics.

This paper summarizes the experimental results of pressure measurements, oil flow, and spatial flowfield, provides the variation of states of the leading-edge vortex system of stack wing for different aspect ratios, and analyzes the effect on aerodynamic characteristics due to vortex twisting and bursting when there is sideslip. Thus, useful data are provided for computing aerodynamic characteristics of flight vehicles.

### III. Experimental equipment

Experiments on force measurements, pressure measurements, space flowfield, and oil flow were conducted at a low-speed wind

tunnel in the Institute of Fluid Mechanics of Brunswick University. The diameter of the experimental section of the wind tunnel is 1.3m; the wind speed was 40m/s, with a Reynolds number of  $1.3 \times 10^6$ . By using a micro type probe and a coordinate instrument, the space flowfield was measured; the measurement plane was perpendicular to the incident flow stream. Spacing between measurement points was 5 percent of the wingspan; the spacing was appropriately shortened near the vortex zone. In the oil flow experiments, a mixture of titanium oxide, vegetable oil, and acetic acid was used. During the experiments, a vortex detector was employed to qualitatively detect the positions of the vortex axis and the bursting point.

The stream display was carried out at a water tunnel at the institute; the experimental section dimensions were 0.25m x 0.33m; the flow speed was 0.2m/s; and the Reynolds number was  $2.5 \times 10^4$ . Blue ink was the display agent.

The experimental model was a plate stack wing, as shown in Fig. 1. Holes for pressure measurements were at the locations 0.75 and 0.875 times the root chord from the apex of the aircraft wing.

### III. Experimental Results

#### 1. Aircraft with aspect ratio 2.05

Fig. 2 shows the states of the vortex system at both sides of the aircraft wing for different angles of attack and sideslip angles by integrating the flow display, space flowfield, and pressure measurements as found experimentally. At small sideslip

angles, the vortex system on the wing surface can be obviously divided into three zones. At small angles of attack, both sides of the wing surface are, respectively, two separated vortices.

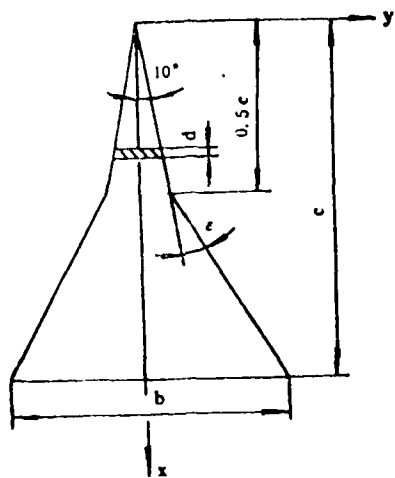


Fig. 1. Model

展弦比 a	e	风洞模型 mm			水洞模型 mm		
		c	b	d	c	b	d
3.01	30°	500	507.7	3	125	126.9	1
2.05	20°	500	376.6	3	125	94.2	1
1.31	10°	500	270.2	3	125	67.5	1

KEY: a - Aspect ratio    b - Wing tunnel model, in mm    c - Water tunnel model, in mm

At increasing angles of attack, the intensities of the front and rear vortices become higher; induction between the two vortices grows; the front and the rear vortices twist and merge on the wing surface. When the angle of attack is greater than a certain value (related to sideslip angle), the twisted vortex bursts at the wing surface. Sideslip reduces the effective sweptback angle at the upstream side of the wing. The spacing between the front

vortex and rear vortex becomes larger; the twisting between the two vortices is delayed but the twisted vortex is easy to burst. The phenomena are exactly the reverse at the downstream side. At large sideslip angles, the wing surface vortex system is relatively complex. At the upstream side, the intensities of the front vortex and rear vortex further weaken; before the two vortices twist, the rear vortex is the first to burst. However, at larger angles of attack, both vortices twist first before bursting. At the downstream side, since the front vortex is further from the wing surface, these two vortices do not twist. When the angle of attack is very large, the rear vortex and the front vortex successively burst on the wing surface.

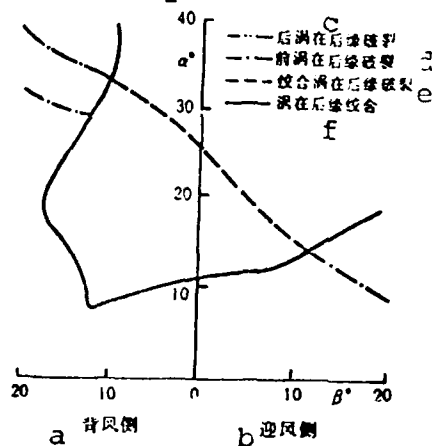


Fig. 2. Vortex system for stack wing with aspect ratio 2.05  
KEY: a - Downstream side b - Upstream side  
c - Bursting of rear vortex at the downstream edge d - Bursting of front vortex at the downstream edge  
e - Bursting of twisted vortex at downstream edge f - Twisting of vortices at the trailing edge

Fig. 3 shows the variation curves of coefficients of lift, dip and elevation moments, as well as rolling moment for

$\alpha = 12^\circ, 16^\circ, \text{ and } 30^\circ$ . The hatched lines in the figure show the influence of vortex twisting and bursting corresponding to Fig. 2. When the angle of attack is  $12^\circ$  and the sideslip angle is  $5^\circ$ , two vortices at the upstream side of the wing just twist at the trailing edge. With an increase in the sideslip angle, the twisted vortex again separates on the wing surface; the influence range of the vortex becomes greater; and a positive additional lift is obtained by the wing. Based on the functioning position of the additional lift, the aircraft wing receives the additional pitch-down moment and a negative additional rolling moment. When the angle of attack is  $12^\circ$  and the sideslip angle is  $13^\circ$ , the twisted vortex at the downstream side of the aircraft wing again separates into two vortices. Since the front vortex is farther from the wing surface, the influence of the vortex near the trailing edge at the downstream side becomes weaker; the wing receives a negative additional lift, a pitch-up additional moment, and a negative additional rolling moment. At the angle of attack  $16^\circ$  and sideslip angle  $7.5^\circ$ , the twisted vortex at the upstream of the wing bursts at the trailing edge. With an increase in sideslip angle, the bursting point of the vortex moves upstream; the influence of the vortex near the trailing edge of the upstream side weakens. Thus, the aircraft wing receives a negative additional lift, a pitch-up additional moment, and a positive rolling moment. At the angle of attack  $16^\circ$  and sideslip angle  $16^\circ$ , with increase in sideslip angle, the vortex system varies at the downstream side

of the aircraft wing and the aerodynamic forces also vary; these variations are similar to the case at angle of attack  $12^\circ$  and sideslip angle  $13^\circ$ . At angle of attack  $30^\circ$  and sideslip angle  $4^\circ$ , the twisted vortex at the downstream of the aircraft wing bursts at the trailing edge. With increase in sideslip angle, the vortex bursting point moves downstream; the influence of the vortex near the trailing edge at the downstream side becomes stronger. Thus, the aircraft wing receives a positive additional lift, a pitch-down additional moment, and a positive additional rolling moment. At angle of attack  $30^\circ$  and sideslip angle  $12^\circ$ , variations in the vortex system and in the aerodynamic forces at the downstream of the aircraft wing are analogous to the case of angle of attack  $12^\circ$  and sideslip angle  $13^\circ$ . From Fig. 3, the vortex twisting or separation have a weaker influence on aerodynamic characteristics; however, vortex bursting has a stronger influence on the aerodynamic characteristics.

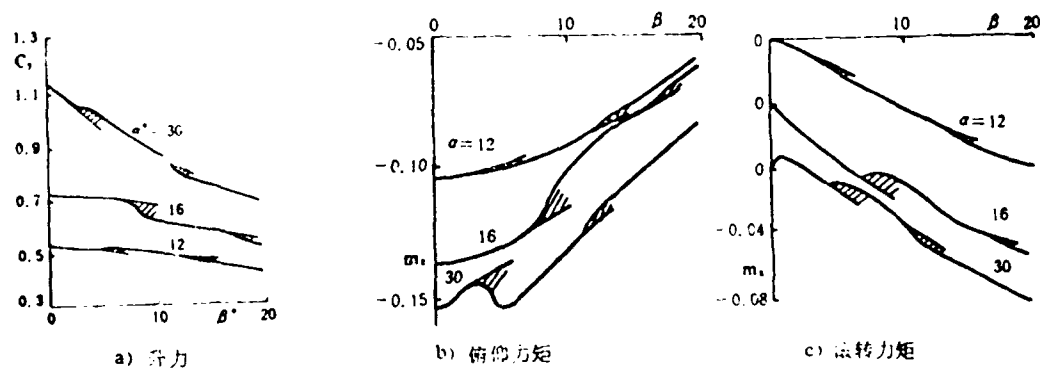


Fig. 3. Aerodynamic characteristics of stack wing with aspect ratio 2.05

LEGEND: a - Lift    b - Pitch-down and pitch-up moments  
c - Rolling moment

## 2. Aircraft wings at aspect ratio 1.31 and 3.01

Figs. 4 and 5 show the states of the vortex system at different angles of attack and different sideslip angles for wings at aspect ratios 1.31 and 3.01. After comparison with Fig. 2, at increasing aspect ratios, the spacing between the front vortex and the rear vortex becomes greater; the intensity of the rear vortex weakens. The trend toward twisting of the two vortices weakens, but the vortices burst easily. Therefore, the nontwisting zone on the wing surface for the two vortices expands; two vortices twist but the zone in which the vortices do not yet burst shrinks, but the vortex bursting zone grows larger. At higher aspect ratios, variations in vortex system states becomes complex. Noteworthy is the situation near the  $0^\circ$  sideslip angle for the aircraft wing with aspect ratio 3.01. When the angle of attack is in the vicinity of  $7^\circ$ , the rear vortex has already burst at the trailing edge. With a further increase in the angle of attack to approximately  $11^\circ$ , the rear vortex is again restored to the state of not bursting. This is possibly due to the fact that there is increased induction on the rear vortex at increasing angles of attack and intensifying front vortex.

## IV. Results

The article summarizes the experimental results of force and pressure measurements of stack wings, as well as the flow display. The vortex system states of a sideslip stack wing with different aspect ratios are given; the influence on the

aerodynamic characteristics of the aircraft wing due to vortex twisting and vortex bursting are analyzed. The results indicate the following.

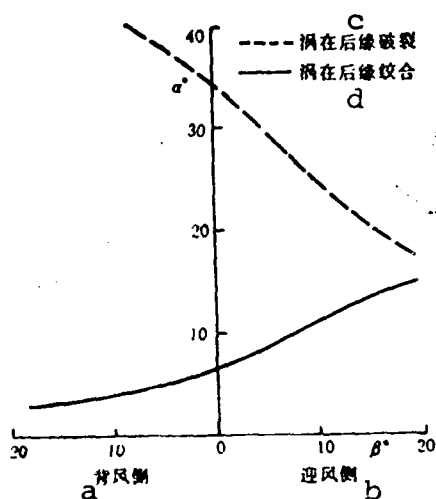


Fig. 4. Vortex system for stack wing with aspect ratio 1.31  
KEY: a - Downstream side  
b - Upstream side c - Vortex bursting at trailing edge  
d - Vortex twisting at trailing edge

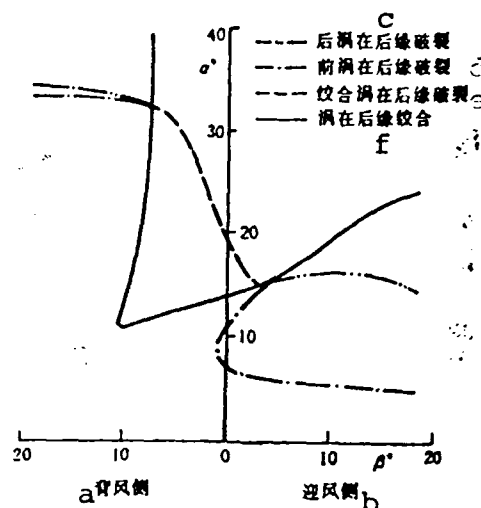


Fig. 5. Vortex system of stack wing of aspect ratio 3.01  
KEY: a - Downstream side  
b - Upstream side  
c - Bursting of rear vortex at trailing edge  
d - Bursting of front vortex at leading edge  
e - Bursting of twisted vortex at trailing edge  
f - Twisting of vortex at trailing edge

1. The planform of the aircraft wing has a considerable influence on the state of the vortex system. Without varying the stack shape and at higher aspect ratios, the shape of the vortex system on the wing surface grows in complexity; vortices are not easy to twist, but a twisted vortex bursts readily.

2. At increasing sideslip angles, vortex twisting at the upstream side of the aircraft wing is delayed; the vortex bursts

easily. The phenomena at the downstream are exactly the reverse.

3. Vortex bursting has a stronger influence on aerodynamic characteristics; the influence due to vortex twisting is weaker.

The first draft of the paper was received on 23 November 1987; the revised draft was received for publication on 28 January 1988.

#### REFERENCES

- [1] Wentz, W.H. and McMahon, M.C., NASA CR-714, (1967).
- [2] Hoeijmakers, H.W.M. and Vaatstra, W., AIAA 82-0949, (1982).
- [3] Verhaagen, N.G., AGARD CP-342, (1983), 7-1~7-16.

DISTRIBUTION LIST

DISTRIBUTION DIRECT TO RECIPIENT

<u>ORGANIZATION</u>	<u>MICROFICHE</u>
B085 DIA/RTS-2FT	1
C509 BALLOC509 BALLISTIC RES LAB	1
C510 R&T LABS/AVEADCOM	1
C513 ARRADCOM	1
C535 AVRADCOM/TSARCOM	1
C539 TRASANA	1
Q592 FSTC	4
Q619 MSIC REDSTONE	1
Q008 NTIC	1
Q043 AFMIC-IS	1
E051 HQ USAF/INET	1
E404 AEDC/DOF	1
E408 AFWL	1
E410 ASDTC/IN	1
E411 ASD/FTD/TTIA	1
E429 SD/IND	1
P005 DOE/ISA/DDI	1
P050 CIA/OCR/ADD/SD	2
1051 AFTT/LDE	1
P090 NSA/CDB	1
2206 FSL	1

Microfiche Nbr: FTD93C000468  
FTD-ID(RS)T-0034-93